

OPEN

pK_a of opioid ligands as a discriminating factor for side effects

Giovanna Del Vecchio^{1,4}, Dominika Labuz^{1,4}, Julia Temp^{1,4}, Viola Seitz¹, Michael Kloner¹, Roger Negrete¹, Antonio Rodriguez-Gaztelumendi^{1,3}, Marcus Weber², Halina Machelska¹ & Christoph Stein^{1*}

The non-selective activation of central and peripheral opioid receptors is a major shortcoming of currently available opioids. Targeting peripheral opioid receptors is a promising strategy to preclude side effects. Recently, we showed that fentanyl-derived μ -opioid receptor (MOR) agonists with reduced acid dissociation constants (pK_a) due to introducing single fluorine atoms produced injury-restricted antinociception in rat models of inflammatory, postoperative and neuropathic pain. Here, we report that a new double-fluorinated compound (FF6) and fentanyl show similar pK_a, MOR affinity and [³⁵S]-GTP γ S binding at low and physiological pH values. *In vivo*, FF6 produced antinociception in injured and non-injured tissue, and induced sedation and constipation. The comparison of several fentanyl derivatives revealed a correlation between pK_a values and pH-dependent MOR activation, antinociception and side effects. An opioid ligand's pK_a value may be used as discriminating factor to design safer analgesics.

Opioids are the strongest drugs used for the treatment of pain, but serious problems have emerged due to their epidemic misuse and adverse effects (reviewed in¹). Systemically applied conventional opioid agonists activate both central and peripheral opioid receptors (reviewed in^{2–4}) and elicit major side effects such as sedation, respiratory depression, nausea, addiction, tolerance and constipation (reviewed in^{1,5}). Targeting peripheral opioid receptors is a promising strategy to reduce adverse effects (reviewed in⁶). An increasing number of animal and clinical studies indicate that a large proportion of analgesia evoked by systemically administered opioids is mediated by such peripheral receptors^{7–12}.

Many painful syndromes are associated with injury-induced tissue acidosis (reviewed in⁶) and low extracellular pH increases opioid agonist efficacy by altering the activation of opioid receptors and possibly G proteins^{3,13–15}. In previous studies, we developed a novel artificial intelligence-based design of opioids lacking central or intestinal side effects by selectively targeting opioid receptors in the acidic environment of peripheral injured tissue. This approach aims at reducing a ligand's pK_a by introducing electronegative fluorine atoms in order to preclude the protonation of its tertiary amine (an essential prerequisite for opioid receptor activation) at pH 7.4 (in brain and intestinal wall)^{3,15,16}. In contrast to established wisdom that the pK_a of a drug affects pharmacokinetic characteristics such as absorption, distribution, metabolism and excretion (ADME)¹⁷, our novel concept is based on the different pharmacodynamics of opioid ligand-receptor interactions under physiological versus pathological conditions. However, the optimal pK_a to minimize side effects is not known to date. In this study, we tested the newly designed double-fluorinated compound *N*-{1-[2-(2,6-difluorophenyl)ethyl]piperidine-4-yl}-*N*-phenylpropionamide (FF6), and examined whether successively decreasing an opioid ligand's pK_a values correlates with the loss of central and intestinal side effects.

Results

Design, synthesis, and pK_a determination of FF6. Conventional fentanyl has an experimentally determined pK_a value of 8.44 ± 0.05 ¹⁸. To introduce electronegative moieties and facilitate chemical synthesis, two hydrogens were replaced by two fluorine atoms at the phenyl ring in the fentanyl structure (Fig. 1). Accordingly, FF6 was synthesized by a contractor (ASCA GmbH Berlin, Germany) and its pK_a was experimentally measured as 7.94 ± 0.01 by another contractor (Sirius Analytical Ltd., Forest Row, UK). This compound was compared

¹Charité - Universitätsmedizin Berlin, Campus Benjamin Franklin, Department of Experimental Anesthesiology, Hindenburgdamm 30, 12203, Berlin, Germany. ²Zuse Institute Berlin, Computational Molecular Design, Takustraße 7, 14195, Berlin, Germany. ³Present address: Department of Drug Discovery and In Vitro Pharmacology, Laboratorios Dr. Esteve, Parc Científic de Barcelona, Baldiri Reixac 4-12, Barcelona, Spain. ⁴These authors contributed equally: Giovanna Del Vecchio, Dominika Labuz and Julia Temp. *email: Christoph.stein@charite.de

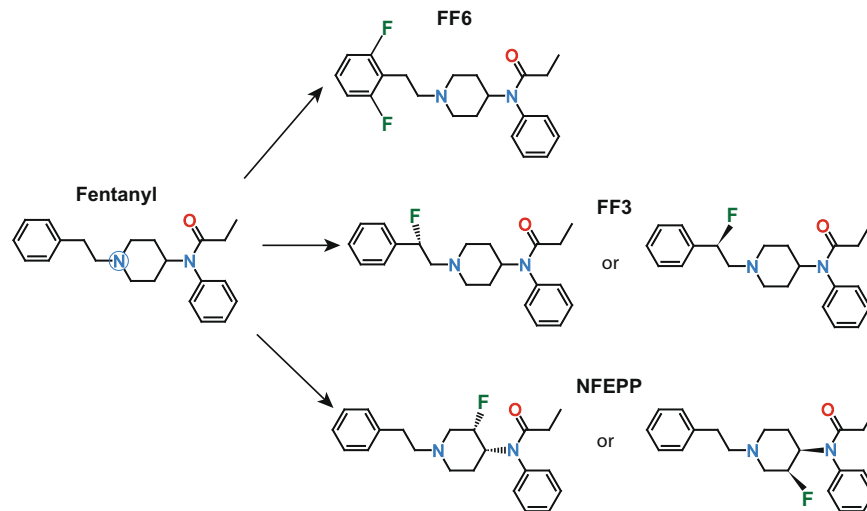


Figure 1. Chemical structures of fentanyl, *N*-[1-[2-(2,6-difluorophenyl)ethyl]piperidine-4-yl]-*N*-phenylpropionamide (FF6), (\pm)-*N*-[1-(2-fluoro-2-phenylethyl)piperidine-4-yl]-*N*-phenyl propionamide (FF3) and (\pm)-*N*-(3-fluoro-1-phenylethylpiperidine-4-yl)-*N*-phenyl propionamide (NFEPP). The blue circle highlights the tertiary nitrogen atom subjected to pH-dependent protonation in whose vicinity electrons may be withdrawn to reduce the pK_a value. The respective isomers of FF3 and NFEPP are shown. Sites of fluorination are indicated as F.

to fentanyl and two previously described derivatives (\pm)-*N*-[1-(2-fluoro-2-phenylethyl)piperidine-4-yl]-*N*-phenyl propionamide (FF3) and (\pm)-*N*-(3-fluoro-1-phenylethylpiperidine-4-yl)-*N*-phenyl propionamide (NFEPP) (Fig. 1).

FF6 binds to and activates μ -opioid receptors (MOR) at both low and physiological pH. In binding experiments on membrane preparations of MOR-transfected human embryonic kidney 293 (HEK 293) cells, FF6 showed similar potency (IC_{50}) to displace the radioactively-labeled standard MOR ligand [3H]-[D-Ala²,N-Me-Phe⁴,Gly⁵-ol]-enkephalin (DAMGO) (4 nM) at pH 6.5 and physiological pH 7.4 (Fig. 2A,B and Table 1). In the [^{35}S]-GTP γ S binding assay, both the maximum effects and the EC_{50} values of FF6 were similar at pH 6.5 and at pH 7.4 (Fig. 2C,D and Table 1).

FF6 produces antinociception in healthy and injured tissue. To assess antinociceptive efficacy, we used a clinically relevant rat model of pain, unilateral complete Freund's adjuvant (CFA)-induced hindpaw inflammation¹⁹. Four days following intraplantar (i.pl.) CFA injection, rats developed mechanical hyperalgesia indicated by reduced paw pressure thresholds (PPT) in ipsilateral compared to contralateral paws, and to thresholds before injury (Fig. 3). Intravenous (i.v.) fentanyl (Fig. 3A,B) and FF6 (Fig. 3C,D) (4–16 μ g/kg) produced dose-dependent antinociception manifested by increased PPT at 10–30 min after injection. These effects occurred both in inflamed (Fig. 3A,C) and contralateral, noninflamed paws (Fig. 3B,D). To examine the contribution of central vs. peripheral opioid receptors, we used subcutaneous (s.c.) administration of naloxone hydrochloride (NLX) and bilateral intraplantar (i.pl.) injection of naloxone methiodide (NLXM). These opioid receptor antagonists do²⁰ or do not cross the blood-brain barrier²¹, respectively. The antinociceptive effects produced by fentanyl and FF6 (each at 16 μ g/kg, i.v.) in inflamed paws were completely suppressed to the baseline thresholds before injections by NLX (2 mg/kg) (Fig. 3E,I). In contrast, the antinociception induced by both agonists was only partially abolished by NLXM (50 μ g), as manifested by significantly different effects compared to baseline thresholds (Fig. 3F,J). The effects evoked by both agonists in contralateral, noninflamed paws were fully reversed by NLX to the baseline thresholds (Fig. 3G,K), but were not altered by NLXM, as demonstrated by the lack of significant differences compared with animals treated with both agonists and vehicle (Fig. 3H,L).

FF6 induces central and intestinal side effects. Next, we examined typical opioid side effects mediated centrally (sedation) or intestinally (constipation), as determined by locomotor activity and defecation, respectively. Both fentanyl and FF6 (each at 30 μ g/kg, s.c.) decreased locomotor activity, measured as the distance traveled within 30 min after drug injections (Fig. 4A), and reduced defecation (Fig. 4B).

pK_a values correlate with side effects. Finally, we gathered some *in vitro* and *in vivo* data from our previous studies^{3,15,18} to enable the direct comparison of the effects of all four compounds in physiological (pH 7.4) and acidic environments. FF6 ($pK_a = 7.94$) and fentanyl ($pK_a = 8.44$) showed similar MOR affinity and [^{35}S]-GTP γ S binding at both pH 6.5 and 7.4 (Table 1). FF3 ($pK_a = 7.22$) showed significantly enhanced potency to displace [3H]-DAMGO binding (i.e. increased MOR affinity) at low pH (Table 1). In the [^{35}S]-GTP γ S assay, both the maximum effect and the EC_{50} of FF3 were lower at pH 6.5 than at pH 7.4 (Table 1). NFEPP ($pK_a = 6.82$) displayed significantly enhanced MOR binding and showed a tendency to increase G-protein activation at pH 6.5 compared to pH 7.4 (Table 1). *In vivo*, FF6 and fentanyl (the ligands with high pK_a) produced significantly elevated PPT over

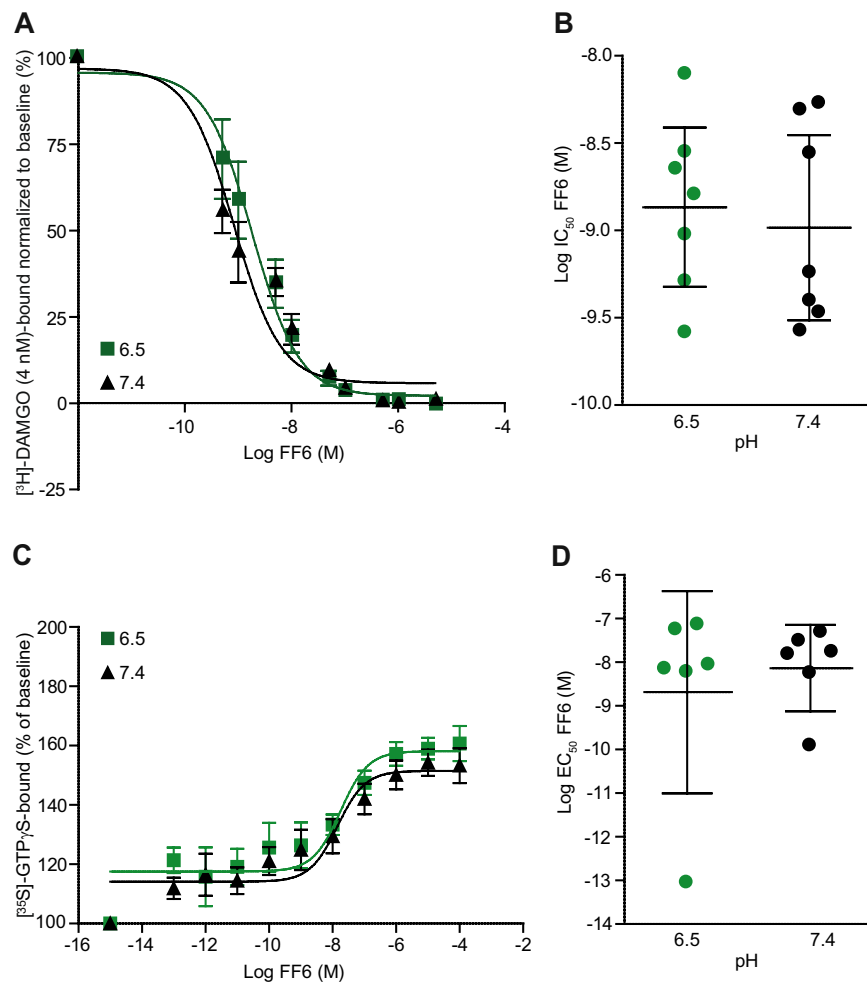


Figure 2. Binding and activation of MOR. (A) Displacement of bound [³H]-DAMGO (4 nM) by FF6 at pH 6.5 and 7.4. (B) IC₅₀ calculated from (A). $P > 0.05$, unpaired t -test ($n = 6-7$). (C) [³⁵S]-GTP-γS binding induced by FF6 at pH 6.5 and 7.4. [³⁵S]-GTP-γS binding is expressed as percent increase in [³⁵S]-GTP-γS binding relative to binding in unstimulated samples ($n = 6$). (D) EC₅₀ of FF6 from (C). $P > 0.05$, unpaired t -test. Data are presented as mean \pm SEM (A, C) and as mean \pm 95% confidence intervals (B, D) ($n = 6$).

| Drug | Calculated pK _a | Experimentally obtained pK _a | MOR binding (IC ₅₀ nM) in HEK 293 cells | | Maximum [³⁵ S]-GTP-γS binding at 100 μM agonist (% of baseline) | | EC ₅₀ of [³⁵ S]-GTP-γS binding (nM) | |
|----------|----------------------------|---|--|--------------------------------|---|------------------|--|---------------------------------|
| | | | pH 6.5 | pH 7.4 | pH 6.5 | pH 7.4 | pH 6.5 | pH 7.4 |
| Fentanyl | 9.11 ³ | 8.44 \pm 0.05 ¹⁸ | 6.9 \pm 1.1 ¹⁵ | 4.8 \pm 0.7 ¹⁵ | 157.7 \pm 9.1 | 144.1 \pm 2.9 | 125.5 \pm 20.6 ³ | 96.1 \pm 16.6 ³ |
| FF6 | n/a | 7.94 \pm 0.01 | 2.3 CI: -0.1 to 4.6 | 2.0 CI: -0.002 to 4.1 | 157.3 \pm 3.9 | 151.3 \pm 4.4 | 22.8 CI: -6.8 to 52.4 | 17.9 CI: 1 to 34.8 |
| FF3 | 6.01 ³ | 7.22 \pm 0.01 ³ | 7.1 \pm 1.4 ³ | 48.3 \pm 6.4 ^{***3} | 129.9 \pm 11.6 | 164.9 \pm 21.4 | 47.2 \pm 24.2 ³ | 231.4 \pm 47.9 ^{**3} |
| NFEPP | 6.83 ¹⁵ | 6.82 \pm 0.06 ¹⁵ | 18.3 \pm 3.3 ¹⁵ | 81.9 \pm 22.1 ^{*15} | 149.4 \pm 10.6 | 137.7 \pm 2.4 | 131.4 \pm 29.8 | 337.7 \pm 166.1 |

Table 1. Comparison of *in vitro* effects of compounds with different pK_a values. Data are represented as mean \pm SEM (for normally distributed data) or mean with 95% confidence intervals (for non-normally distributed data). N.S., not significant $P > 0.05$; * $P < 0.05$; ** $P < 0.01$; *** $P < 0.0001$; Mann-Whitney or unpaired t -test ($n = 6-8$); n/a: n.

baselines (antinociception) both in inflamed and noninflamed paws (Fig. 3A–D; elevated AUC in Fig. 5A,B). In contrast, NFEPP and FF3 (the ligands with low pK_a) did not affect noninflamed paws (AUC close to zero; Fig. 5B) and evoked antinociception only in inflamed paws (Fig. 5A) (all substances at 4–12 μg/kg, i.v.). Sedation and constipation were observed only after administration of the ligands with high (FF6, fentanyl) but not with low pK_a values (FF3, NFEPP) (all at 30 μg/kg, s.c.; Fig. 5C,D).

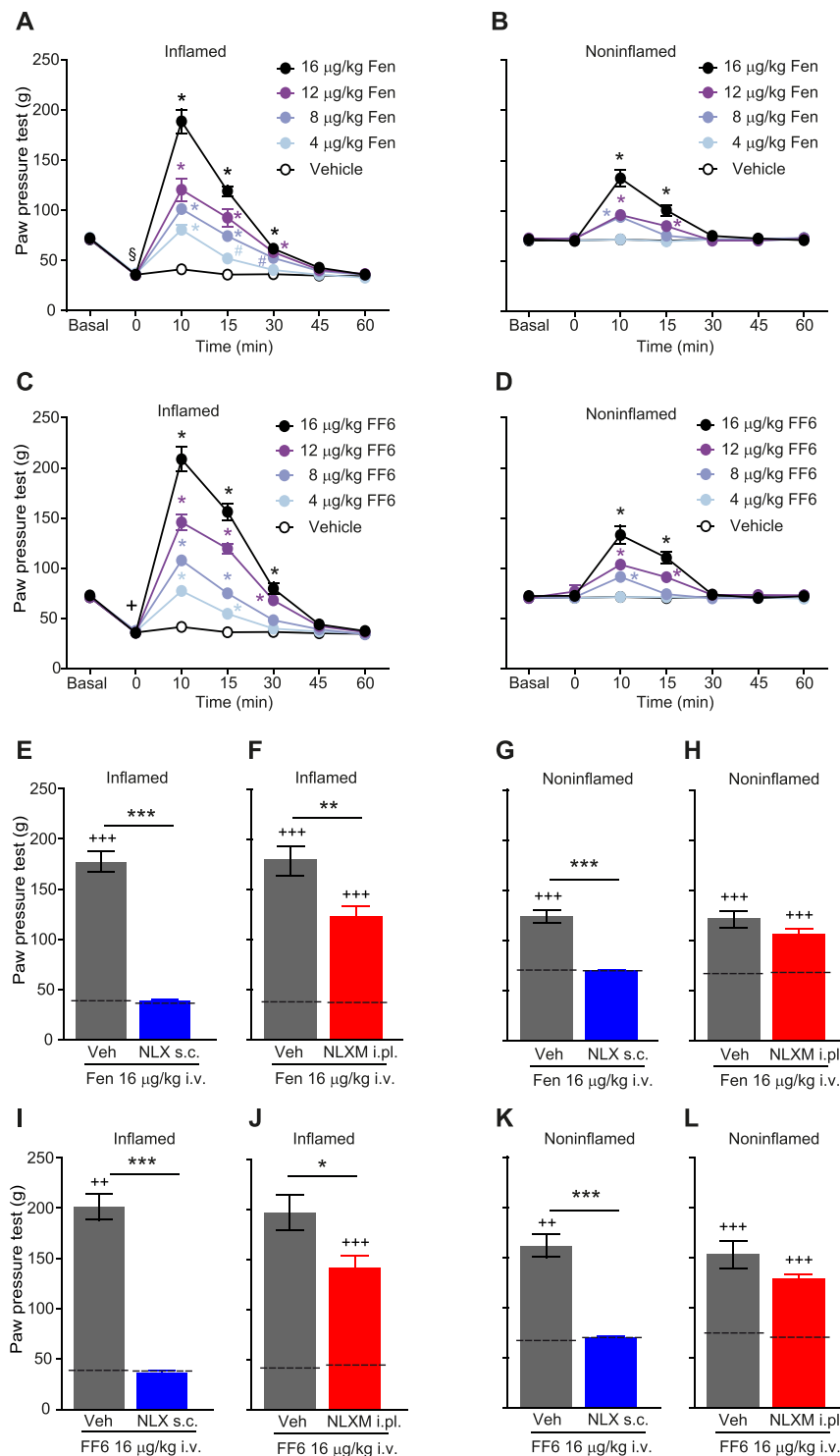


Figure 3. Antinociceptive effect of systemic FF6 in the unilateral CFA-induced hindpaw inflammation. (A–D) Elevation of PPT after intravenous (i.v.) injection of fentanyl (Fen) (A,B) and FF6 (C,D) in inflamed (A,C) and noninflamed (B,D) hindpaws, assessed before (Basal) and 4 days after i.p. CFA application (0) at 10 to 60 min after injection of fentanyl or FF6. $^{\circ}P < 0.01$, $^{\circ}P < 0.001$ vs: corresponding baseline threshold (Basal) before CFA injections, paired *t*-test or Wilcoxon test; $^*P < 0.05$, $^{**}P < 0.001$ vs. vehicle, two-way RM ANOVA and Bonferroni test ($n = 8-10$). (E–L) Effects of antagonists on PPT elevations produced 10 min after i.v. injection of fentanyl (E–H) or FF6 (I–L) (each at 16 µg/kg). Naloxone hydrochloride (NLX, 2 mg/kg) or vehicle (Veh) were injected subcutaneously (s.c.) (E,G,I,K). Naloxone methiodide (NLXM, 50 µg) or vehicle (Veh) were injected intraplantarly (i.pl.) into both hindpaws (F,H,J,L). $^*P < 0.05$, $^{**}P < 0.01$, $^{***}P < 0.001$ NLXM or NLX + Fen or FF6 vs. Veh + Fen or FF6, unpaired *t*-test; $^{+++}P < 0.01$, $^{++++}P < 0.0001$ vs. corresponding baseline thresholds (dashed lines) evaluated 4 days after CFA, but before any injections; paired *t*-test or Wilcoxon test ($n = 10$ animals per condition for all except vehicle in J and L ($n = 8$)). Data are presented as mean \pm SEM.

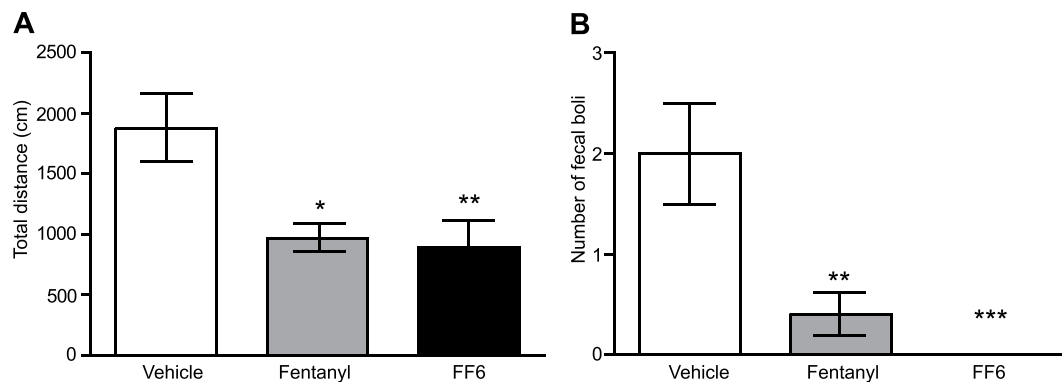


Figure 4. Central and intestinal side effects induced by systemic fentanyl and FF6. **(A)** Effects of subcutaneous (s.c.) fentanyl and FF6 (each at 30 $\mu\text{g}/\text{kg}$) on locomotion, expressed as the total distance (in cm) travelled during 30 min after drug injection. * $P < 0.05$, ** $P < 0.01$ vs. vehicle, one-way ANOVA and Dunnett's test. **(B)** Effects of fentanyl and FF6 on constipation presented as the number of defecations during 1 h after s.c. fentanyl or FF6 injection. ** $P < 0.01$, *** $P < 0.001$ vs. vehicle, Kruskal-Wallis ANOVA and Dunn's test. Data are presented as mean \pm SEM ($n = 10$ animals per condition).

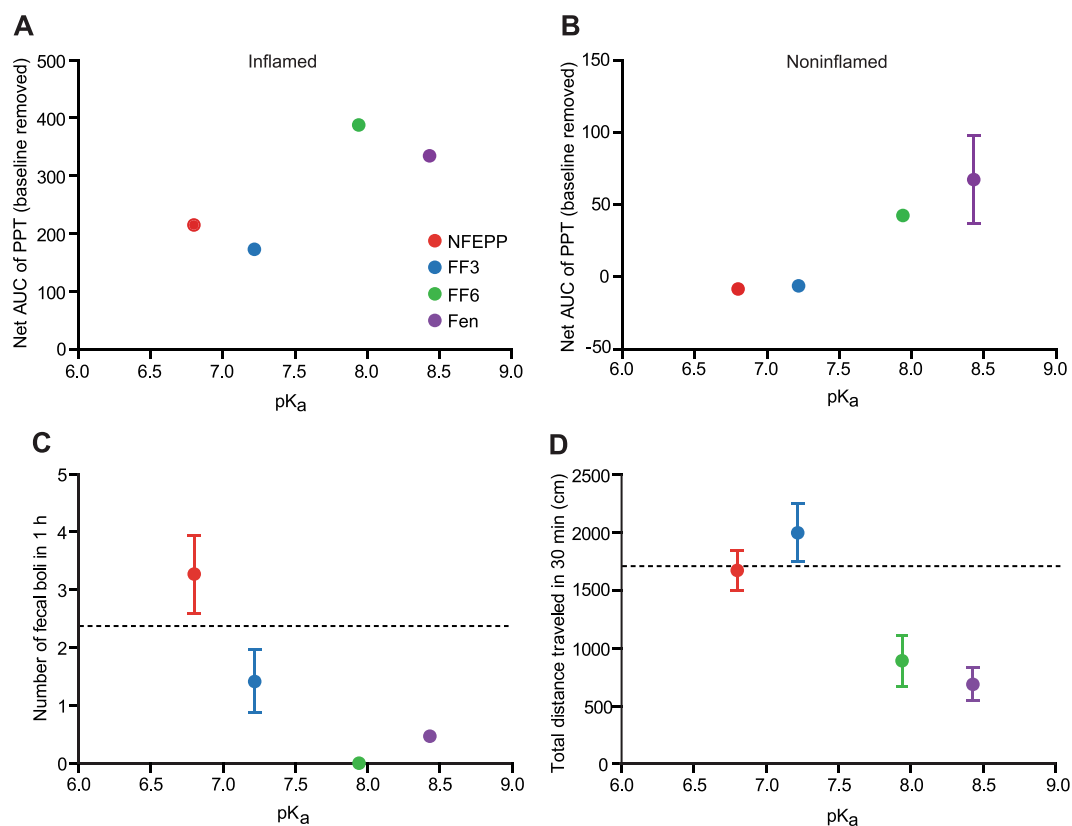


Figure 5. Correlation between pK_a values of compounds with antinociception and side effects. **(A,B)** Antinociceptive effects as net $\text{AUC}_{(4-12 \mu\text{g}/\text{kg})}$ of PPT (negative values result from subtraction of pre-CFA baseline PPT) at 15 min after i.v. injection of NFEPP, FF3, FF6 and Fen in inflamed **(A)** and contralateral, noninflamed **(B)** paws. AUC values were derived from curves generated by use of $n = 9$ (NFEPP and FF3 from^{3,15}), $n = 8-10$ (FF6, see also Fig. 3) and $n = 19$ (Fen) animals. **(C)** Constipation, as assessed by number of fecal boli 1 h after s.c. injection of agonists (30 $\mu\text{g}/\text{kg}$) in relation to the pK_a of the substance. Maximum and minimum numbers (with 95% confidence intervals) of boli in controls (vehicle-treated) are shown by the dashed line. Fen ($n = 30$) and controls ($n = 34$) (always included in all experiments) are averaged across all experiments; NFEPP ($n = 11$); FF3 ($n = 12$); FF6 ($n = 10$). **(D)** Locomotor activity as assessed by the total distance travelled during 30 min after s.c. injection of agonists (30 $\mu\text{g}/\text{kg}$) in relation to the pK_a of the substance. Maximum and minimum travelled distances (with 95% CI) in controls (vehicle-treated) are shown by the dashed line. Fen ($n = 31$) and controls ($n = 34$) (always included in all experiments) are averaged across all experiments; NFEPP ($n = 10$); FF3 ($n = 12$); FF6 ($n = 10$). Graphs show means \pm SEM (where available).

Discussion

The activation of opioid receptors in peripheral inflamed (acidic) tissue is a promising strategy to reduce injury-induced pain and avoid central and intestinal side effects (reviewed in⁶). Conventional opioid agonists have pK_a values above 7.5 (reviewed in³). Therefore, their protonation and the subsequent activation of opioid receptors occur at both physiological and low pH^{3,15}. Using computational simulations, we recently demonstrated that replacing a single hydrogen by a fluorine atom within a distance of two carbon bonds from the tertiary amine in the fentanyl molecule decreased the pK_a values of two derivatives (NFEPF, FF3) and promoted their selective protonation in inflamed tissue^{3,15,16}. This led to enhanced potency of MOR ligands at low pH *in vitro*, a finding that was confirmed by Dockendorff and colleagues²². In the current study, we examined a new compound created by replacing two hydrogens with two fluorine atoms at the phenylethyl ring (FF6).

The comparison of the four ligands revealed that the pK_a of FF6 (7.94) was higher than physiological pH and closer to the pK_a of fentanyl (8.44) than to the pK_a of FF3 (7.22) or NFEPF (6.82). Apparently, the newly introduced fluorine atoms were not able to sufficiently reduce pK_a . This might be due to the already high electronegativity of the phenyl ring itself, or to the larger distance (four carbon bonds) between the fluorine atoms and the tertiary amine in FF6 than in NFEPF or FF3 (Fig. 1).

Consistent with their high pK_a values, FF6 and the standard MOR opioid agonist fentanyl induced comparable MOR binding and G-protein activation at both physiological and low pH, which is likely due to their similar protonation status under all pH conditions. In contrast, FF3 ($pK_a = 7.22$) and NFEPF ($pK_a = 6.82$) showed enhanced opioid binding and G-protein activation under acidic conditions, indicating that an increased proton concentration improved the interaction between ligands and opioid receptors.

When analyzing *in vivo* effects in correlation to pK_a values, we found that the ligands with high pK_a values (FF6, fentanyl) produced antinociception in both inflamed and in contralateral, non-inflamed paws, whereas the compounds with low pK_a (FF3, NFEPF) were inactive in noninflamed tissue. To discriminate between central and peripheral sites of action, we used s.c. NLX and i.pl. NLXM. The applied sites, doses and times of injection were based on previous studies that had shown that, at those modes of administration, NLX blocks both central and peripheral opioid receptors, whereas NLXM blocks only peripheral opioid receptors^{15,23,24}. While systemic NLX abolished the effects of FF6 and fentanyl bilaterally, locally administered NLXM partially reduced only the effects in inflamed paws. In addition, both FF6 and fentanyl induced sedation and constipation. Together, these data indicate that FF6 and fentanyl activate both central (NLX-accessible) and peripheral (NLX- and NLXM-accessible) opioid receptors. These findings are consistent with our *in vitro* data and with the notion that both FF6 and fentanyl are protonated and capable of activating MOR at physiological (in brain or intestinal wall) as well as low pH (at the site of peripheral inflammation). Because we found no significant advantage of FF6 over conventional fentanyl, we did not further explore respiratory effects or addiction potential.

These results support our hypothesis that ligands with pK_a values close to the pH of inflamed/injured tissue selectively activate peripheral opioid receptors. The lack of pK_a reduction and the resulting absence of pH- and injury-specific action of FF6 confirmed this hypothesis. When comparing the present results with our previous *in vivo* studies on FF3 and NFEPF¹⁵, it appears that progressively decreasing pK_a values correlate with reduced sedation and constipation (Fig. 5C,D). Importantly, these experiments were conducted over a period of only two years under identical conditions in our laboratory by the same investigators. Although the results are reported in separate publications, we do not consider this a comparison of new with historical data or a limitation of the analysis. Of note, our approach does not exploit drug distribution, e.g. the entry into the brain or intestinal wall. In contrast to the known influence of the pK_a on a drug's pharmacokinetic characteristics such as absorption or distribution¹⁷, our concept is based on the different pharmacodynamics of opioid ligand-receptor interactions under physiological versus pathological conditions. The chemical structures of our fluorinated derivatives are very close to fentanyl, a highly lipophilic molecule. Therefore, we expect the tissue distribution of NFEPF, FF3 and FF6 to be similar to fentanyl. As systemically administered fentanyl is known to rapidly enter the brain²⁵, we assume that all substances are able to enter central and peripheral compartments. This will have to be verified in future investigations. However, as we have shown, the likelihood of producing adverse side effects by activating off-target opioid receptors at normal pH values (in brain, intestinal wall or other non-injured tissue) declines with decreasing pK_a values of agonists. Therefore, an opioid ligand's pK_a value might be used as discriminating factor in the design of safer analgesics.

Methods

Chemicals/Drugs. Fentanyl citrate, NLX, NLXM, guanosine 5'-[γ -thio]triphosphate tetralithium salt (cold GTP γ S) and guanosine 5'-diphosphate sodium salt (GDP) were purchased from Sigma-Aldrich (Taufkirchen, Germany). [³H]-DAMGO and [³⁵S]-GTP γ S were purchased from Perkin Elmer (Rodgau-Jügesheim, Germany). Isoflurane was purchased from AbbVie (Ludwigshafen, Germany), and CFA was purchased from Calbiochem (La Jolla, CA, USA).

FF6 (base) was synthesized by a contractor (ASCA GmbH, Berlin, Germany) (Fig. 1). The experimental measurement of pK_a was performed by a contractor (Sirius Analytical Ltd., Forest Row, UK). For *in vitro* experiments, fentanyl and FF6 were initially dissolved in water and dimethyl-sulfoxide (DMSO), respectively, and diluted in assay buffer to final concentrations. For *in vivo* experiments, FF6 was dissolved in DMSO and diluted with 0.9% NaCl to obtain the final concentrations. The maximum DMSO concentration was 4.2% for s.c., and 0.5% for i.v. injections. Fentanyl, NLX and NLXM were dissolved in water and diluted with 0.9% NaCl. Control groups were treated with vehicle (DMSO or NaCl, respectively). In the previously described fentanyl derivatives, fluorination of the ethylidene bridge yielded FF3 (experimental $pK_a = 7.22$)³, and fluorination of the piperidine ring led to the compound NFEPF (experimental $pK_a = 6.82$)¹⁵ (Fig. 1 and Table 1).

Cell cultures. HEK 293 cells (wild type or stably expressing rat MOR) were maintained in DMEM media (Sigma-Aldrich) supplemented with 10% fetal bovine serum and 1% penicillin/streptomycin in the absence or presence of 0.1 mg/ml geneticin (Biochrom AG, Berlin, Germany), respectively, in 5% CO₂ at 37 °C. Depending on their density, cells were passaged 1:3–1:10 every second to third day from P8 to P28²⁶.

Radioligand binding assays. MOR-expressing HEK 293 cells were cultured in flasks with a growth area of 175 cm². Cells were washed twice with ice-cold assay buffer (Trizma[®] Preset Crystals, 50 mM, pH 7.4) (Sigma-Aldrich), then harvested from the culture flask in 10 ml ice-cold assay buffer, homogenized and centrifuged twice at 42,000 g for 20 min at 4 °C as described previously^{24,27,28}. Protein concentration was determined according to the Bradford method²⁹. The half-maximal inhibitory concentration (IC₅₀) of FF6 required to displace 4 nM of the standard MOR ligand [³H]-DAMGO was determined at pH values 6.5 and 7.4. A protein amount of 100 µg was incubated with 4 nM [³H]-DAMGO (50 Ci/mmol) and FF6 dissolved in 50 mM assay buffer at pH 6.5 or 7.4 for 90 min at room temperature. Nonspecific binding was determined by the addition of 10 µM NLX²⁴. Filters were soaked in 0.1% polyethyleneimine solution before use. Bound and free ligands were separated by rapid filtration under vacuum through Whatman GF/B glass fiber filters. Bound radioactivity was determined by liquid scintillation spectrophotometry at 69% counting efficiency for [³H] after overnight extraction of the filters in scintillation fluid.

For [³⁵S]-GTPγS-binding experiments, membranes were prepared as described above. After determination of protein concentration, membranes were centrifuged as described above and resuspended in [³⁵S]-GTPγS-binding assay buffer (100 mM NaCl, 50 mM Tris Base, 5 mM MgCl₂, 0.1 mM EGTA, 0.2% bovine serum albumin, 10 mM dithiothreitol and 0.03 mM GDP) adjusted to pH 7.4 or 6.5³⁰. A protein amount of 50 µg was incubated with 0.05 nM [³⁵S]-GTPγS and varying concentrations of fentanyl derivatives at the respective pH for 2 h at 30 °C to determine dose response curves and EC₅₀ values. Whatman GF/B glass fiber filters were soaked in water before use. Bound and free [³⁵S]-GTPγS was separated *via* rapid filtration as described above. Nonspecific binding was determined by the addition of 10 µM cold GTPγS. Basal [³⁵S]-GTPγS-binding was measured in the absence of opioid ligand and cold GTPγS.

Animals. Experiments were performed in male Wistar rats (200–300 g, 6–7 weeks old, Janvier Laboratories, France) and approved by the State animal care committee (Landesamt für Gesundheit und Soziales, Berlin). All procedures were conducted in accordance with the ARRIVE guidelines³¹ and with the ethical guidelines of the International Association for the Study of Pain. Animals were randomly assigned to treatment or control groups for behavioral experiments. The experimenters were blinded to the doses and drug treatments. Rats were kept on a 12 h dark-light cycle in groups of 2–3 in cages lined with ground corncob bedding with free access to food and water *ad libitum*, and at constant room temperature (22–24 °C) and humidity (60–65%). Before nociceptive testing, handling was performed once per day for 4 days for 1–2 min each day. For assessment of locomotor activity, animals were habituated to the test cages one day before the experiment for 15 min. Statistical power calculations were performed to obtain the minimal number of animals for the experiments. After termination of the experiments, rats were killed by an overdose of isoflurane.

Induction of hindpaw inflammation. Rats received an i.pl. injection of CFA (150 µl, 0.1% *Mycobacterium butyricum*) into the right hindpaw under brief isoflurane anesthesia¹⁹. Nociceptive testing was performed before and 4 days after CFA injection.

Injections and experimental protocols. Brief isoflurane anesthesia was applied for i.v. (200 µl) injections. Nociceptive tests were performed in separate groups of animals, before and 5–60 min after drug injections. NLX was injected s.c. immediately before i.v. injection of agonists, similar to our previous study²³. NLXM was injected i.pl. into both hindpaws immediately before i.v. injection of agonists, and pain thresholds were measured 10 min thereafter as described previously²⁴. To avoid interference of general anesthesia with locomotor activity and to allow comparison with our previous studies^{3,15}, subcutaneous (s.c.; 200 µl) injections without anesthesia were used for assessment of the other behavioral parameters. In addition, previous studies showed that ratios of peak plasma concentrations after i.v. versus s.c. administration of opioids were similar, and that these concentrations correlated well with antinociceptive and side effects^{32–35}. All dosages were determined in pilot experiments.

Mechanical hyperalgesia (Randall-Selitto test). Rats were gently held under paper wadding and incremental pressure was applied via a wedge-shaped, blunt piston onto the dorsal surface of the hindpaws using an automated gauge (Ugo Basile, Comerio, Italy). The paw pressure threshold (PPT) necessary to induce paw withdrawal was determined by averaging three consecutive trials separated by 15 s intervals. The cut-off was set at 250 g to avoid tissue damage. The sequence of paws was alternated between animals to preclude order effects.

Locomotor activity. Horizontal locomotor activity of healthy rats was measured in open field plastic cages with dark walls (44 × 44 × 40 cm, without top) (Ugo Basile). Locomotion was recorded by an infrared camera coupled to a computer with AnyMaze Video Tracking System (Stoelting Co. Wood Dale, IL, USA) and was measured as total distance (in cm) travelled during 30 min after s.c. drug administration, analogous to our previous studies^{3,15}.

Defecation. Excreta of individual rats were collected and counted for 1 h after s.c. drug administration in open field plastic cages^{3,15}.

Data handling and statistical analyses. All data were assessed for normal distribution and equal variances by Kolmogorov-Smirnov test and/or D'Agostino and Pearson tests. In dose-response experiments

(displacement binding and GTP γ S-assay), means of values at each agonist concentration and each pH were calculated and used to derive IC₅₀, EC₅₀ and the maximum [³⁵S]-GTP γ S binding by nonlinear regression and were then subjected to unpaired *t*-test for normally distributed data or Mann-Whitney test for non-normally distributed data. To enable direct comparison of the *in vitro* effects of all four compounds, we included some data in Table 1 (calculated pK_a of fentanyl, FF3 and NFEPP; experimentally obtained pK_a of FF3 and NFEPP, MOR binding of fentanyl, FF3 and NFEPP; EC₅₀ of FF3) that were generated in our previous studies^{3,15}. Behavioral data were expressed as raw values or transformed to area under the curve (AUC). The net AUC_(4–12 μg/kg) values were obtained by calculating the area between the X-axis and the dose-dependency curve of the PPT at 15 min after application of i.v. fentanyl, NFEPP, FF3 or FF6 at doses of 4, 8 and 12 μg/kg. The data presented in Fig. 5 (antinociception and side effects produced by fentanyl, FF3 and NFEPP) were gathered from our previous studies^{3,15}, except for FF6 (this study). Notably, the peak effects of fentanyl, FF6 and NFEPP were observed at 10 min¹⁵ (this study), while those of FF3 were measured at 15 min after injections³. To enable direct comparison, we decided to use the effects of all compounds at 15 min after injection. At this time point, fentanyl, FF6 and NFEPP still significantly elevated PPT in inflamed (fentanyl, FF6, NFEPP) and non-inflamed paws (fentanyl, FF6). Transformed data (AUC) were not subjected to statistical analysis. Two-sample comparisons of raw values were made using paired or unpaired *t*-test for normally distributed data, or Wilcoxon or Mann-Whitney test for non-normally distributed data. Changes over time (more than two time points) after one treatment were evaluated using one-way repeated measures (RM) ANOVA followed by Bonferroni test for normally distributed data, or Friedman one-way RM ANOVA followed by Dunn's test for non-normally distributed data. Two-way RM ANOVA and Bonferroni or Tukey's test were used to compare two parameters over time. Multiple comparisons at one time point were performed using one-way ANOVA followed by Dunnett's test or Bonferroni test for normally distributed data, or by Kruskal Wallis one-way ANOVA followed by Dunn's test for non-normally distributed data. Differences were considered significant if P < 0.05. Prism 5 (GraphPad, San Diego, USA) was used for all tests and graphs and data were expressed as means ± standard error of the mean (SEM) or means ± 95% confidence intervals (Fig. 2B,D and Table 1).

Received: 17 July 2019; Accepted: 3 December 2019;

Published online: 18 December 2019

References

- Rutkow, L. & Vernick, J. S. Emergency Legal Authority and the Opioid Crisis. *N Engl J Med* **377**, 2512–2514 (2017).
- Del Vecchio, G., Spahn, V. & Stein, C. Novel Opioid Analgesics and Side Effects. *ACS Chem Neurosci* **8**, 1638–1640 (2017).
- Spahn, V. *et al.* Opioid receptor signaling, analgesic and side effects induced by a computationally designed pH-dependent agonist. *Sci Rep* **8**, 8965 (2018).
- Stein, C. Opioid Receptors. *Annu Rev Med* **67**, 433–451 (2016).
- Califf, R. M., Woodcock, J. & Ostroff, S. A Proactive Response to Prescription Opioid Abuse. *N Engl J Med* **374**, 1480–1485 (2016).
- Stein, C. New concepts in opioid analgesia. *Expert Opin Investig Drugs* **27**, 765–775 (2018).
- Shannon, H. E. & Lutz, E. A. Comparison of the peripheral and central effects of the opioid agonists loperamide and morphine in the formalin test in rats. *Neuropharmacology* **42**, 253–261 (2002).
- Furst, S. *et al.* Peripheral versus central antinociceptive actions of 6-amino acid-substituted derivatives of 14-O-methyloxymorphone in acute and inflammatory pain in the rat. *J Pharmacol Exp Ther* **312**, 609–618 (2005).
- Labuz, D., Mousa, S. A., Schafer, M., Stein, C. & Machelska, H. Relative contribution of peripheral versus central opioid receptors to antinociception. *Brain Res* **1160**, 30–38 (2007).
- Jagla, C., Martus, P. & Stein, C. Peripheral opioid receptor blockade increases postoperative morphine demands—a randomized, double-blind, placebo-controlled trial. *Pain* **155**, 2056–2062 (2014).
- Shinohara, A., Andoh, T., Saiki, I. & Kuraishi, Y. Analgesic effects of systemic fentanyl on cancer pain are mediated by not only central but also peripheral opioid receptors in mice. *Eur J Pharmacol* **833**, 275–282 (2018).
- Sun J., Chen S. R., Chen H., Pan H. L. mu-Opioid receptors in primary sensory neurons are essential for opioid analgesic effect on acute and inflammatory pain and opioid-induced hyperalgesia. *J Physiol* (2018).
- Selley, D. E., Breivogel, C. S. & Childers, S. R. Modification of G protein-coupled functions by low-pH pretreatment of membranes from NG108-15 cells: increase in opioid agonist efficacy by decreased inactivation of G proteins. *Mol Pharmacol* **44**, 731–741 (1993).
- Vetter, I., Kapitzke, D., Hermanussen, S., Monteith, G. R. & Cabot, P. J. The effects of pH on beta-endorphin and morphine inhibition of calcium transients in dorsal root ganglion neurons. *J Pain* **7**, 488–499 (2006).
- Spahn, V. *et al.* A nontoxic pain killer designed by modeling of pathological receptor conformations. *Science* **355**, 966–969 (2017).
- Rodriguez-Gaztelumendi, A., Spahn, V., Labuz, D., Machelska, H. & Stein, C. Analgesic effects of a novel pH-dependent mu-opioid receptor agonist in models of neuropathic and abdominal pain. *Pain* **159**, 2277–2284 (2018).
- Manallack, D. T. The pK(a) Distribution of Drugs: Application to Drug Discovery. *Perspect Medicin Chem* **1**, 25–38 (2007).
- Thurkill, R. L., Cross, D. A., Scholtz, J. M. & Pace, C. N. pK_a of fentanyl varies with temperature: implications for acid-base management during extremes of body temperature. *J Cardiothorac Vasc Anesth* **19**, 759–762 (2005).
- Stein, C., Millan, M. J. & Herz, A. Unilateral inflammation of the hindpaw in rats as a model of prolonged noxious stimulation: alterations in behavior and nociceptive thresholds. *Pharmacol Biochem Behav* **31**, 445–451 (1988).
- Markowitz, R., Jacobson, J., Bain, G. & Kornetsky, C. Naloxone blockade of morphine analgesia: a dose-effect study of duration and magnitude. *J Pharmacol Exp Ther* **199**, 385–388 (1976).
- Brown, D. R. & Goldberg, L. I. The use of quaternary narcotic antagonists in opiate research. *Neuropharmacology* **24**, 181–191 (1985).
- Rosas, R. Jr., Huang, X. P., Roth, B. L. & Dockendorff, C. beta-fluorofentanyls are pH-sensitive mu-opioid receptor agonists. *ACS Med Chem Lett* **10**, 1353–1356 (2019).
- Stein, C., Millan, M. J., Yassouridis, A. & Herz, A. Antinociceptive effects of mu- and kappa-agonists in inflammation are enhanced by a peripheral opioid receptor-specific mechanism. *Eur J Pharmacol* **155**, 255–264 (1988).
- Gonzalez-Rodriguez, S. *et al.* Polyglycerol-opioid conjugate produces analgesia devoid of side effects. *Elife* **6**, 1–24 (2017).
- Green, P. G. & Kitchen, I. Different effects of di-isopropylfluorophosphate on the entry of opioids into mouse brain. *Br J Pharmacol* **84**, 657–661 (1985).
- Spahn, V. *et al.* Opioid withdrawal increases transient receptor potential vanilloid 1 activity in a protein kinase A-dependent manner. *Pain* **154**, 598–608 (2013).
- Busch-Dienstfertig, M., Roth, C. A. & Stein, C. Functional characteristics of the naked mole rat mu-opioid receptor. *PLoS One* **8**, e79121 (2013).

28. Shaqura, M. A., Zollner, C., Mousa, S. A., Stein, C. & Schafer, M. Characterization of mu opioid receptor binding and G protein coupling in rat hypothalamus, spinal cord, and primary afferent neurons during inflammatory pain. *J Pharmacol Exp Ther* **308**, 712–718 (2004).
29. Bradford, M. M. A rapid and sensitive method for the quantitation of microgram quantities of protein utilizing the principle of protein-dye binding. *Anal Biochem* **72**, 248–254 (1976).
30. Ludwig, M. G. *et al.* Proton-sensing G-protein-coupled receptors. *Nature* **425**, 93–98 (2003).
31. Kilkenny, C., Browne, W. J., Cuthill, I. C., Emerson, M. & Altman, D. G. Improving bioscience research reporting: the ARRIVE guidelines for reporting animal research. *Osteoarthritis Cartilage* **20**, 256–260 (2012).
32. Chiavaccini, L. *et al.* Pharmacokinetics and pharmacodynamics comparison between subcutaneous and intravenous butorphanol administration in horses. *J Vet Pharmacol Ther* **38**, 365–374 (2015).
33. KuKanich, B. Pharmacokinetics of subcutaneous fentanyl in Greyhounds. *Vet J* **190**, e140–142 (2011).
34. Lee, H. K., Lebkowska-Wieruszewska, B., Kim, T. W., Kowaski, C. J. & Giorgi, M. Pharmacokinetics of the novel atypical opioid tapentadol after intravenous, intramuscular and subcutaneous administration in cats. *Vet J* **198**, 620–624 (2013).
35. Ranheim, B. *et al.* Pharmacokinetics of pethidine in pigs following intravenous, intramuscular and subcutaneous administration. *J Vet Pharmacol Ther* **21**, 491–493 (1998).

Acknowledgements

We thank Prof. H. Schick and Dr. C. Wedler (ASCA GmbH) for continuous consulting on chemistry, N. Vogel for technical assistance, and O. Perepelica for stimulating discussions on computational simulations. This work was supported by Bundesministerium für Bildung und Forschung (VIP 0272/03V0364). The Charité-Universitätsmedizin Berlin and the Zuse Institute Berlin have filed patents on pH-dependent opioid receptor agonists (US 9133120 B2) and computational methods (PCT/EP2013/102681). C.S. was supported by *Charité 3^R | Replace-Reduce-Refine*.

Author contributions

C.S. and M.W. conceived the original idea. M.W. designed the chemical structures. V.S. (née Spahn), G.D.V., J.T., D.L., M.K., R.N., A.R.G., H.M., and C.S. designed, performed, and/or analyzed *in vitro* and behavioral data. G.D.V., D.L., J.T., V.S., M.W., H.M. and C.S. contributed to writing the paper.

Competing interests

C.S. and M.W. are listed as inventors on US patent 14/239,461 and EP 2,801,046. The other authors declare no competing financial or non-financial interests.

Additional information

Correspondence and requests for materials should be addressed to C.S.

Reprints and permissions information is available at www.nature.com/reprints.

Publisher's note Springer Nature remains neutral with regard to jurisdictional claims in published maps and institutional affiliations.



Open Access This article is licensed under a Creative Commons Attribution 4.0 International License, which permits use, sharing, adaptation, distribution and reproduction in any medium or format, as long as you give appropriate credit to the original author(s) and the source, provide a link to the Creative Commons license, and indicate if changes were made. The images or other third party material in this article are included in the article's Creative Commons license, unless indicated otherwise in a credit line to the material. If material is not included in the article's Creative Commons license and your intended use is not permitted by statutory regulation or exceeds the permitted use, you will need to obtain permission directly from the copyright holder. To view a copy of this license, visit <http://creativecommons.org/licenses/by/4.0/>.

© The Author(s) 2019